WILEY
Publishers Since 1807

GSK3β regulates oligodendrogenesis in the dorsal microdomain of the subventricular zone via Wnt-β-catenin signaling

SCHOLARONE™
Manuscripts

John Wiley & Sons, Inc.

GSK3β regulates oligodendrogenesis in the dorsal microdomain of the subventricular zone via Wnt-β-catenin signalling

Kasum Azim[1,2], Andrea Rivera[1], Olivier Raineteau[2,3], *Arthur M Butt[1]

[1]Institute of Biomedical and Biomolecular Sciences, School of Pharmacy and Biomedical Science, University of Portsmouth, St Michael's Building, White Swan Road, Portsmouth PO1 2DT, UK.

[2]Neuromorphology, Brain Research Institute, University of Zürich / ETHZ, Zürich, Switzerland

[3]Stem-cell and Brain Research Institute, INSERM U846, Lyon, France

*Corresponding author:

Keywords: oligodendrocyte precursor; subventricular zone; glycogen synthase kinase 3β; Wnt; neural stem cells.

Number of pages: 29 (including references)

Word Count: Total - 7317 (including references);   Abstract - 195; Introduction - 430; Methods - 1309; Results - 1719; Discussion – 1116.

Figures: 6

ABSTRACT

Oligodendrocytes, the myelinating cells of the CNS, are derived postnatally from oligodendrocyte precursors (OPs) of the subventricular zone (SVZ). However, the mechanisms that regulate their generation from SVZ neural stem cells (NSC) are poorly understood. Here, we have examined the role of glycogen synthase kinase 3β (GSK3β), an effector of multiple converging signalling pathways in postnatal mice. The expression of GSK3β by rt-qPCR was most prominent in the SVZ and in the developing white matter, around the first 1-2 weeks of postnatal life, coinciding with the peak periods of OP differentiation. Intraventricular infusion of the GSK3β inhibitor ARA-014418 in mice aged postnatal day (P) 8-11 significantly increased generation of OPs in the dorsal microdomain of the SVZ, as shown by expression of cell specific markers using rt-qPCR and immunolabelling. Analysis of stage specific markers revealed that the augmentation of OPs occurred via increased specification from earlier SVZ cell types. These effects of GSK3β inhibition on the dorsal SVZ were largely attributable to stimulation of the canonical Wnt/β-catenin signalling pathway over other pathways. The results indicate GSK3β is a key endogenous factor for specifically regulating oligodendrogenesis from the dorsal SVZ microdomain under the control of Wnt-signalling.

INTRODUCTION

Oligodendrocytes (OLs) are the myelinating cells of the CNS and are essential for normal salutatory conduction. OLs in the postnatal forebrain are derived from oligodendrocyte precursors (OPs) that originate from neural stem cells (NSCs) within the subventricular zone (SVZ) of the lateral ventricle (LV). NSCs first give rise to cycling neural progenitors (NPs) (also known as Type-C cells), identified by their expression of the transcription factor (TF) Mash1 and S-phase markers, which then differentiate into OPs or olfactory neurons (Kessaris et al. 2006; Marshall et al. 2005; Menn et al. 2006; Nakatani et al. 2013; Richardson et al. 2006). The mechanisms regulating SVZ-derived OP specification from Type-C cells are unresolved, but are believed to involve specific environmental and transcriptional and cascades (He and Lu 2013). Postnatally, there is evidence that OPs are derived primarily from the dorsal SVZ (dSVZ), whereas the lateral SVZ (lSVZ) has the greatest neurogenic potential for olfactory neurons (Brill et al. 2009; Kessaris et al. 2006; Marshall et al. 2005; Menn et al. 2006; Young et al. 2007). Recent studies shed new light on the instructive basis of NSC identities in dSVZ and lSVZ microdomains. For example, FGF2 increases OP proliferation in the dSVZ and ectopically in the lSVZ microdomains during development and into adulthood (Azim et al. 2012b). These findings complement our recent study showing an early postnatal role for Wnt-β-catenin signaling in regulating NSC specification and oligodenrogenesis in the dorsal SVZ (Azim et al., 2014), whereas in the adult SVZ Wnt3a strongly increases OL proliferation in the dSVZ without affecting lineage choice or proliferation within neurogenic clones (Ortega et al. 2013).

Glycogen synthase kinase 3β (GSK3β) is a potent negative regulator of multiple signalling pathways in neuronal development, most notably Wnt/β-catenin, as well as Shh and Notch1 (Grimes and Jope 2001; Kim et al. 2011). In unstimulated cells, GSK3β primes β-catenin for destruction and in the presence of canonical Wnt ligands, β-catenin translocates to the nucleus to target specific sets of genes associated with Wnt-signalling (Doble and Woodgett 2003). Since canonical Wnt/β-catenin signalling appears to regulate OL and NP generation in the early postnatal SVZ (Azim et al., 2014), but only OLs in the adult SVZ (Ortega et al., 2013), we wished to determine the mechanisms of GSK3β and Wnt/β-catenin on OPs and NPs during the peak of oligodendrogenesis from the postnatal SVZ in the second week postnatal. The results show that at P8-11, the major period of OL generation in subcortical white matter (Azim et al., 2011), GSK3β/Wnt/β-catenin is a major determinant of OL generation specifically in the dorsal microdomain of the SVZ.

4

MATERIALS AND METHODS

Animals

Mice aged postnatal day (P)8-11 were used throughout. All animal procedures were performed in accordance with the UK Home Office Animals Scientific Procedures Act (1984). Wild-type mice (C57/BL6) were used and transgenic mice of C57/BL6 background in which fluorescent reporters were driven by Sox10–EGFP mice to identify OPs and OLs as previously characterised (Azim et al. 2012b).

In vivo injections

Pups of similar size litters were used throughout. Intraventricular injections of the GSK3β inhibitor ARA-014418 (Bhat et al. 2003) were performed daily for 3 days commencing at P8 and brains examined at P11, as previously described (Azim and Butt 2011). In brief, mice were deeply anaesthetised under isofluorane and ARA-014418 (Sigma-Aldrich) was delivered into the cerebrospinal fluid of the LV using a Hamilton syringe, at a point 2 mm from the midline along the Bregma, and to a depth of 2 mm. ARA-014418 was stored in DMSO, and diluted in sterile saline vehicle and delivered in a volume of 2 μl; sterile saline/DMSO vehicle was used as controls and referred to as controls only throughout. The growth factors PDGF-AA, IGF1 and FGF2 were used at 5 μg/ml in volumes of 2 μl, as in our previous studies (Azim et al. 2012b; Butt et al. 1997; Goddard et al. 1999). The growth factors Wnt3a, EGF and BMP4 were used at 2.5 μg/ml in volumes of 2 μl, in accordance with their effective *in vitro* concentrations in NSC cultures (Lie et al. 2005), and accounting for the dilution effects of injected agents (Azim and Butt 2011). Shh was injected at 100 μg/ml in a

volume of 2 µls, as previously reported (Jiao and Chen 2008). Wnt3a, BMP4, IGF1, PDGF-AA and EGF were obtained from R&D Systems, Shh was obtained from eBiosciences and FGF2 obtained from Peprotech, USA.

Immunohistochemistry

Published protocols were followed for immunolabelling (Azim and Butt 2011; Azim et al. 2012b). In brief, brains were immersion fixed in 4% paraformaldehyde and coronal vibratome sections of 20 µm to 100 µm thickness were cut through the periventricular forebrain. Primary antibodies used were: rabbit anti-PDGFαR (1:400, gift from Prof Stallcup; or 1:100, Abcam); goat anti-PDGFRα(1:200, R&D Systems); rat anti-MBP (1:300, Millipore); mouse anti-Nestin (1:300, BD Biosciences); rabbit anti-Nestin (1:300, R&D Systems); rabbit anti-GFAP (1:300, DAKO); mouse anti-nuclear pβ-Catenin (1:300, Abcam); goat anti-Tyr216-pGSK3β (1:100, Santa Cruz); goat anti-Ser9-pGSK3β (1:100, Santa Cruz); mouse anti-PCNA (1:400, Sigma-Aldrich); mouse anti-Mash1 (1:200, BD Biosciences). Appropriate species-matched secondary antibodies conjugated with Alexafluor 488, 568 or 405 (1:500, Molecular Probes) were used. Primary antibodies of different origin were diluted together in blocking buffer and co-dilutions of the appropriate secondary antibodies were used. Control experiments were performed using appropriate blocking peptides where available or otherwise by omission of the primary antibody. For PCNA or Mash1 labelling, antigen retrieval was performed, whereby free-floating sections were pre-treated with PBST and NP-40 1% for 20 mins to permeate the sections, and following washes in PBS, sections were immersed in pre-boiled citric acid and heated in a commercial microwave pressure cooker at full power for 30 sec for 2

cycles. For nuclear β-catenin, Ser9-pGSK3β, and Tyr216-pGSK3β, treated brains were fixed for 3 hrs in Histochoice Fixative (Sigma-Aldrich). PBS was replaced by TBS (0.5M Tris Base, 9% NaCl, pH 8.4) throughout, to reduce non-specific labeling of anti-phospho antibodies. For pGSK3β detection, sections were incubated in Proteinase K (20 µg/ml in TBS, Invitrogen) for 20 mins at 37ºC followed by incubation in 1% SDS for 1 hr at RT and several washing steps. After final washes in PBS, tissues were mounted on poly-lysine coated glass slides with Vectashield mounting media (Vector Laboratories) and sealed with coverslips. Images were acquired using an LSM 5 Pascal Axioskop2 or LSM 510 meta confocal microscope (Zeiss). Fluorescence was visualized at 488nm (green), 568nm (red) and 405nm (blue) using argon, HeNe1 and diode lasers respectively, using a x40 oil immersion lens with high numerical aperture (1.3nm).

Cell counts

Rostral periventricular coronal sections containing the LV were analysed ($\geq$3 sections per brain, n$\geq$4 animals per group) at rostro-caudal axis 0.6 – 0.9 relative to the Bregma; counts of OL and OP cell numbers confirmed that there were no significant differences between sections in untreated controls (Azim and Butt 2011; Azim et al. 2012b). Images were processed with Zeiss LSM Image Examiner (V. 5.2.0.121), maintaining the acquisition parameters constant to allow comparison between samples. Coronal sections were used throughout and cell counts performed in the dSVZ, lSVZ andcorpus callosum/periventricular white matter on flattened confocal *z*-stacks, of 230 µm^2 x 230 µm^2 in the *x-y*-plane, and 30 µm in the *z*-plane. Extracellular markers were quantified via a nuclear counterstain (propidium iodide (Sigma-Aldrich) or DAPI (Molecular Probes/Invitrogen)). Counts are expressed as

7

mean (SEM, n≥4) cells per field of view volume (FOV) of 1.6 x10^6 μm^3, where the 'n'

value represents the number of mice and the standard error of the mean (SEM).Cell

counts were tested for significance using GraphPad Prism v302, for unpaired t-test

(referred to as t-test) or ANOVA followed by Bonferroni's posthoc test as appropriate.

SVZ microdissection and gene expression profiling

Published protocols were followed for microdissection of the SVZ microdomains and

subsequent RNA procedures (Azim et al. 2012b). ARA-014418 or saline/DMSO was

injected into the LV as above at P8 and at P9 animals were sacrificed ~2.5 hrs after

last treatment by cervical dislocation. A litter of pups were pooled to yield 1 'n' value.

Primers used were: GAPDH, forward CAGCAATGCATCCTGCACC reverse

TGGACTGTGGTCATGAGCCC; Mash1 forward, GACTTTGGAAGCAGGATGG,

reverse GCTGTCTGGTTTGTTTGTTTC; Axin2: forward

GGGGGAAAACACAGCTTACA, reverse ACTGGGTCGCTTCTCTTGAA; Fzdl1:

forward CAAGGTTTACGGGCTCATGT, reverse GTAACAGCCGGACAGGAAAA;

GSK3β: forward GTGGTTACCTTGCTGCCATC, reverse

GACCGAGAACCACCTCCTTT; ABCG2 forward,

CTCAACCTGCCCATTTCAAATGCT, Reverse GTTGGA

AGTCGAAGAGCTGCTGAGA; Nestin

ForwardTACAGGACTCTGCTGGAGGCTGAGA, Reverse

CTGGTATCCCAAGGAAATGCAGCTT; Cyclin D1 Forward

CTGGATGCTGGAGGTCTGTGAGG, Reverse CTGCAGGCGGCTCTTCTTCAAG;

Lef1 Forward, CGTCACACATCCCGTCAGATGTC, Reverse

TGGGTGGGGTGATCTGTCCAACG; Axin2 Forward

GGGGGAAAACACAGCTTACA, Reverse ACTGGGTCGCTTCTCTTGAA; Olig2

Forward GACGATGGGCGACTAGACA, Reverse CAGCGAGCACCTCAAATCTA;

PDGFRα Forward AGAAAATCCGATACCCGGAG, Reverse

AGAGGAGGAGCTTGAGGGAG; Sox4 Forward GAACGGAATCTTGTCGCTGT

; Reverse GAACGCCTTTATGGTGTGGT. ID2 Forward

CTCCTGGTGAAATGGCTGAT, Reverse GCTTATGTCGAATGATAGCAAAG,

STAT1 Forward TCTGAATATTTCCCTCCTGGG, Reverse

CGGAAAAGCAAGCGTAATCT; Hes5 Forward TAGTCCTGGTGCAGGCTCTT

, Reverse GCTGCTGGAGCAGGAGTTC; Hes3 Forward

CGCTGGGATGCTGAATTAGT, Reverse GCTGTCTCTCCTTACCGCTG; Hes1

Forward GGTATTTCCCCAACACGCT, Reverse GAAAGATAGCTCCCGGCATT.

Canonical Wnt-target genes were selected from the following resource:http://www.stanford.edu/group/nusselab/cgi-bin/wnt/target_genes. Those of TGFβ/BMP resulting in downstream SMAD signalling activation were selected based on previous studies (Fei et al. 2010; Ota et al. 2002). Primers for Notch1-target gene expression (Hes1, Hes3 and Hes5) were selected based on previous studies in OP cultures (Wu et al. 2012; Zhou and Armstrong 2007). Primer Express 1.5 software was used to design primers and synthesized by Finnzymes. Gene expression data are presented as mean and the SEM, and samples were compared for significance using t-test as above.

SVZ microdissection and western blot

Animals were sacrificed 45 min after the final injection of ARA-014418or vehicle and SVZ microdomains were rapidly microdissected, snap frozen, centrifuged briefly at 4000 x g to obtain tissue pellets for protein extraction in ice cold lysis buffer containing protease inhibitors, as previously described (Azim and Butt 2011). Lysed tissue supernatant was transferred to Ultrafree MC centrifugal spin columns (Millipore) for separation and concentration of protein extracts above 15KDa. Purification of cytoplasmic and nuclear extracts were obtained using the "NE-PER Nuclear and Cytoplasmic Extraction" kit (Thermo Fisher Scientific, Illinois, US) and

protein concentration determined by Bradford protein assay. Subsequent standard procedures were followed for western blot. Primary antibodies used were: mouse anti-total GSK3β (1:2000, BD Biosciences); mouse anti-nuclear pβ-Catenin (1:1000, Abcam); mouse anti-β-Catenin (1:2000, Abcam); mouse anti-β-actin (1:10000, Sigma-Aldrich); goat anti-Tyr216-pGSK3β (1:500, Santa Cruz); goat anti-Ser9-pGSK3β (1:500, Santa Cruz); mouse anti-Notch1 intracellular cleaved component (NICD) (1:1000, Millipore); rabbit Anti-phospo-SMAD1/5/8 (1:1000, Cell Signaling); Anti-Gli1 (1:1000, Cell Signaling); rabbit Anti-Histone H3 (1:4000; Millipore); rabbit anti-Phospo-Erk1/2 (1:1000, Cell Signaling); mouse anti-total Erk1/2 (1:2000, Cell Signaling). Proteins were visualized by enhanced chemilluminescent detection (Amersham Biosciences), and signal intensities measured via ImageJ software (NIH) and normalised to β-actin or H3 internal controls as appropriate. Experiments were repeated independently at least 3 times and band densitometry values tested for significance using unpaired t-test or ANOVA followed by Bonferroni's posthoc test.

RESULTS

Regional expression and activity of GSK3β in SVZ microdomains

We have shown that GSK3β is implicated in OL differentiation in the developing white matter (Azim and Butt 2011), but it is not clear whether GSK3β regulates the generation of OPs in the postnatal SVZ. To examine this, we determined spatiotemporal differences in GSK3β expression by qPCR of microdissected dSVZ and lSVZ compared to corpus callosum (CC) at differing postnatal ages and in the adult. Transcript levels were normalised against GAPDH housekeeping gene by the comparative $^{\Delta\Delta}$CT method (Azim et al. 2012b) and expression values compared for statistical significance by ANOVA followed by Bonferroni's test (Fig. 1A,B). Overall, spatial expression was greatest in the dSVZ at P4 (Fig. 1A; $p<0.05$), and in the corpus callosum at P8-P11 (Fig. 1A; $p<0.05$). Levels in the corpus callosum fell markedly in the adult (Fig. 1B, $p<0.01$), whereas overall levels were significantly greatest at P8 in both microdomains of the SVZ (Fig. 1B; $p<0.01$), although they remained fairly constant at all ages. The results are consistent with GSK3β being most active during the peak period of OL generation in the postnatal forebrain. We tested this directly by measuring GSK3β activity in the SVZ following infusion of the GSK3β inhibitor ARA-014418, as detailed previously (Azim and Butt, 2011; Azim et al., 2014). GSK3β activity was determined by immunostaining for Ser9-pGSK3β as a marker for the inactive form of GSK3β and Tyr216-GSK3β as a marker for the active form (Cohen and Goedert 2004). Immunostaining demonstrates GSK3β activity in both dSVZ and lSVZ (Fig. 1C-F) in dSVZ OPs (Fig.1G-J), and western blot shows inhibition was significantly greater in the dSVZ microdomain (Fig. 1K, L $p<0.05$, ANOVA followed by Bonferroni's post-hoc test). Two-thirds of OPs in the corpus

callosum, which at this age are derived from the dSVZ (Kessaris et al. 2006),expressed 'active' Tyr216-pGSK3β in controls, and this was significantly decreased following treatment with ARA-014418 (from 64% ± 8% of PDGFRα cells (n=4) to 33.8% ± 6.5% of PDGFRα cells (n=5); p<0.01, t-test), with a concomitant increase in the 'inactive' form Ser9-pGSK3β (from 27.5% ± 3.3% of PDGFRα+ cells in controls (n=4) to 72.3% ± 7.6% of PDGFRα+ cells in ARA-014418 (n=5); p<0.01, t-test). These data show that GSK3β is effectively inhibited by LV infusion of ARA-014418 and demonstrate prominent endogenous GSK3β activity in the SVZ, with greatest activity at P8-11 in the dSVZ microdomain, the time and site of greatest OP generation postnatally. ARA-014418 is not known to have off-target effects on other kinases (Bhat et al. 2003) as described previously (Azim and Butt, 2011; Azim et al., 2014).

GSK3β regulates generation of OPs predominantly from the dSVZ microdomain

The data presented above indicates that GSK3β activity is greatest postnatally in the dSVZ microdomain, which a number of studies indicate is the primary source of OPs that migrate to populate the forebrain during this period (Kessaris et al. 2006). We therefore examined whether GSK3β specifically regulates the generation of OPs in the dSVZ, using transgenic mice in which the lineage-specific transcription factor Sox10 drives the expression of EGFP (Fig. 2). Inhibition of GSK3β with ARA-014418 markedly increased the density of Sox10-EGFP+ cells in the SVZ and surrounding periventricular white matter (PVWM), compared to controls (Fig. 2A, B). Detailed examination of the dSVZ and lSVZ microdomains showed that by far the

predominant effect of GSK3β is on the dSVZ, where Sox10-EGFP+ cells were significantly increased 3-fold (Fig. 2 C, D ,G; p<0.01, t-test), and in the adjacent PVWM (Fig. 2I), compared to a small although statistically significant effect on the lSVZ (Fig. 2 E, F, H). These findings are consistent with GSK3β activity being greatest in the dSVZ microdomain and having a primary role in regulating the generation of OPs from this micodomain, resulting in an increase in the number of OLs in the overlying PVWM.

GSK3β negatively regulates the generation of OPs and neural progenitors (NPs) within specific SVZ microdomains

The results presented above indicate GSK3β activity in the lSVZ, but that its inhibition did not markedly alter OP numbers in this microdomain, suggesting GSK3β mainly regulates OP generation from the dSVZ. Therefore, we next examined the effects of GSK3β inhibition on NSCs and their progeny by qPCR of microdissected microdomains (Fig. 3A-C) and immunostaining (Fig. 4A-D). As described previously (Azim et al. 2012a; Azim et al. 2012b) the SVZ is delineated up to 70 μm from the ependymal wall, based on labelling and aided by nuclear markers. Transcripts enriched in early SVZ cells, ABCG2 and Nestin, were significantly increased by ARA-014418 in both SVZ microdomains, indicative of an increase in NSCs (Fig. 3A; p<0.05, t-test), whereas the NP marker Mash1, and the OP markers Olig2 and PDGFRα were differently altered in the two microdomains (Fig. 3B, C). Transcripts for Mash1, which is expressed by NPs that generate both neurons and OLs, were significantly increased in both microdomains, but the effect was greatest in the dSVZ, where it was barely detectable in controls and reached expression

levels similar to the control lSVZ following GSK3β inhibition (Fig. 3B). In contrast, GSK3β inhibition markedly increased the OL lineage or OP transcripts Olig2 and PDGFRα respectively, by over 3-fold in the dSVZ (Fig. 3C; p<0.01, t-test), with levels in the lSVZ being very low and in the case of PDGFRα not statistically affected by GSK3β inhibition. Immunohistochemical examination of the potential origins of OPs from the dSVZ indicates GFAP+ NSCs and Sox10-EGFP+ cells were segregated populations (Fig.4A,B). In contrast, GSK3β inhibition resulted in striking increases in the dSVZ of Sox10-EGFP co-expression with the NSC/NP marker Nestin (Doetsch et al. 1997) (Fig.4C-E) and the NP marker Mash1 (Fig. 4F-H), consistent with previous reports of early or new OPs expressing Mash1 (Nakatani et al. 2013). Notably, GSK3β inhibition induced a massive expansion in Mash1+ cells dSVZ, and a significant (p<0.001; t-test) three-fold increase in the proportion of Mash1+/Sox10- cells (arrows; Fig. 4G,H). Mash1 expression in OPs is confined to the earliest stage of their differentiation and is transient, hence the large increase in Mash1+/Sox10- cells is consistent with these cells generating the increase in Sox10+/Mash1- OPs (Ortega et al. 2013; Nakatani et al. 2013). The remaining proportion of Mash1+ cells that do not express Sox10-EGFP are Type-C cells and a small fraction of Mash1 expressing neuroblasts (Azim et al. 2012a; Parras et al. 2004; Smith and Luskin 1998)(Azim et al. 2012a; Parras et al. 2004; Smith and Luskin 1998). Double immunolabelling for PDGFRα with PCNA (proliferating cellular nuclear antigen) demonstrated a doubling in PDGFRα+ OP and PDGFRα- cells within the dSVZ following GSK3β inhibition, the latter indicative of potential and likely NSC proliferation (Fig.4 I-K; p<0.001, t-test). These findings indicate that GSK3β regulates the generation of NP in both the dSVZ and lSVZ, while regulating the generation of OP in a region-specific manner. Cell death was examined using propidium iodide

labelling, but in all cases was low in controls and following treatment, in line with our previous study (Azim and Butt et al 2011).

GSK3β differentially regulates multiple targets in SVZ microdomains

GSK3β is known to modulate several signalling pathways in neural development, most notably Wnt and notch1 pathways (reviewed in (Grimes and Jope 2001; Kim and Snider 2011), which we previously showed were mechanisms by which GSK3β regulates OL differentiation in the optic nerve (Azim and Butt 2011). We therefore examined this in the SVZ microdomains using western blot and qPCR (Fig. 5). In the P9 SVZ, cytosolic bound β-catenin was increased in both dSVZ and lSVZ microdomains following ARA-014418 (Fig. 5A, B), whereas nuclear levels of β-catenin were increased to a significantly greater extent in the dSVZ (Fig. 5C, D; $p<0.01$, t-test). Moreover, within cytoplasmic extracts, the levels of Erk1/2 were not affected by ARA-014418, indicating it did not have off target effects on other growth factor-related signalling pathways (Fig. 5A). In addition, we measured nuclear accumulation of the transcription form of Notch1 (NICD), together with BMP signalling via pSMAD1/5/8 and Gli1 for Shh-signalling (Fig. 5C-E). Nuclear levels of activated cleaved Notch1 (NCID) were reduced similarly in both SVZ microdomains ($p<0.05$; t-test), whereas BMP-signalling was only decreased in the dSVZ ($p<0.05$; t-test), and Gli1 was marginally, but significantly, increased in the lSVZ, consistent with greater Shh expression in this microdomain ($p<0.05$, t-test) (Azim et al. 2012b; Palma et al. 2005). These effects were further validated by qPCR of microdissected dSVZ assayed ~2.5 h following ARA-014418infusion (Fig. 5F). Transcripts for β-catenin target genes cyclin D1, Axin2 and Lef1 were all significantly increased by

almost 3-fold in the dSVZ following GSK3β inhibition (Fig. 5F; p<0.01, t-test). By comparison, the Notch1 target Hes3 and Hes5 genes were marginally but statistically significantly downregulated, whereas Hes1 was not statistically altered (p<0.05; t-test), as was the case for BMP signalling - Sox4, ID2, Stat1 (Fig. 5F). These findings suggest that the predominant effect of inhibiting GSK3β in the dSVZ microdomain is largely attributed to the Wnt pathway, with little effect on other pathways that may regulate oligodendrogenesis in the postnatal SVZ.

FGF2 and Wnt3a act by inhibiting GSK3β

The effects of ARA-014418 demonstrate that endogenous GSK3β regulates the generation of OPs in the postnatal SVZ. Several trophic factors are known to regulate NSC fate and OP differentiation, including FGF2 and Wnt (Azim and Butt, 2011; Azim et al., 2012; Azim et al., 2014), and so we examined whether these may act to inhibit GSK3β in a manner similar to ARA-014418 (Fig. 6A, C). Growth factors were infused into the LV of P9 pups and animals sacrificed 45 min later and microdissected dSVZ analysed by western blot of cytosolic extracts for Ser9 pGSK3β. Compared to controls, we found that only FGF2 and Wnt3a inhibited pGSK3β (Fig. 6A, C; p<0.01, test), and we confirmed that Wnt3a and ARA-014418 acted to increase nuclear β-catenin translocation (Fig. 6B, D; p<0.01, t-test), as did FGF2, but to a lesser extent (p<0.05; t-test). In addition, EGF appeared to reduce Ser9 pGSK3β via unknown mechanisms, but this was not examined further. Intriguingly, BMP4 and EGF reduced nuclear β-catenin (p<0.01, t-test) (Fig. 6C, D), whereas other growth factors (IGF1, PDGF-AA and Shh) did not affect pGSK3β or nuclear β-catenin. Hence, inhibition of GSK3β with ARA-014418 primarily mimics the

effects of endogenous canonical Wnts on the dSVZ and to a lesser extent FGF2, consistent with previous findings (Azim et al. 2012b; Azim et al., 2014; Ortega et al. 2013).

DISCUSSION

Multiple cues control the numbers of OPs, but the factors that regulate their generation from germinal SVZ cells is unclear. Here, we show that inhibition of GSK3β with ARA-014418 profoundly stimulated the expansion of NPs in the dSVZ and their differentiation into OPs derived from this microdomain. The results demonstrate that oligodendrogenesis is strongly regulated by GSK3β predominantly in the dSVZ microdomain and suggest that it acts mainly via the canonical Wnt/β-catenin pathway.

The default source of SVZ-derived oligodendrogenesis under specific demyelinating or growth factor conditions appears to be dSVZ (Azim et al. 2012b; Azim et al., 2014), consistent with this microdomain in generating most of the forebrain derived OL lineage cells during postnatal development (Kessaris et al. 2006). Inhibiting GSK3β resulted in the preferential genesis of OL lineage cells from the dSVZ, mirroring our previous observations on Wnt signalling and FGF2 (Azim et al. 2012b; Azim et al., 2014). Furthermore, we provide evidence that FGF2 acts in part to inhibit GSK3β, but not to the same extent as canonical Wnt-signalling. Targeted genetic ablation of GSK3β in NSCs of the developing telencephalon dramatically disrupts neuronal maturation whilst NSCs and cycling NPs are massively upregulated (Kim et al. 2009a). In comparison, targeted β-catenin expression in later OL lineage cells delays their differentiation (Fancy et al. 2009; Ye et al. 2009). In addition, inhibitors for GSK3β have been used previously *in vivo* to assess the role of Wnt-signalling in determining cell fate in the SVZ and in NSCs (Adachi et al. 2007; Azim et al., 2014; Kriks et al. 2011; Maurer et al. 2007). Our findings identify a key role for GSK3β and

Wnt/β-catenin in regulating oligodendrogenesis in the forebrain from the proliferating (Mash1+) NPs in the dSVZ microdomain. Adachi et al. (2007) have shown that the increased proliferation observed in the SVZ results in an increase migration of NPs and OPs. Our results suggest that the same might occur in neonates following inhibition of GSK3β, since we observed an increase number of NPs and OPs at some distance (several hundred micrometers from the SVZ), in particular in the dorsolateral corner where many migrating cells converge. Future fate mapping studies will be necessary to address the fate of the extra numerous OPs being produce after GSK3β inhibition

The SVZ microdomains were assayed by western blot and qPCR for the signalling pathways that mediated the increased oligodendrogenesis regulated by GSK3β. Inhibition of GSK3β increased nuclear translocation of β-catenin specifically in the dSVZ, whereas the activities of Erk1/2, BMP and Shh pathways were not modified, indicating a primary effect on the canonical Wnt/β-catenin signalling, and ruling out possible cross-talk with other growth factor regulated pathways. Moreover, we demonstrated induction of the Wnt target genes Axin2 and Lef1 together with increases in OL lineage markers in the dSVZ following GSK3β inhibition, supporting recent studies on the importance of Wnt-signalling in OP generation from NSC of the doral SVZ microdomain in early postnatal mice (Azim et al., 2014) and adult mice (Ortega et al. 2013). With respect to neurogenesis from the dSVZ and lSVZ, the effects of GSK3β on Notch1, BMPs and Shh signalling pathways are likely to be important (Kim and Snider 2011). The Shh activated transcription factor Gli1 was only induced by GSK3β inhibition in the lSVZ, consistent with higher Shh expression

in this region at P8 (Azim et al. 2012b; Palma et al. 2005). A mechanism exists for GSK3β in negatively regulating downstream Shh signalling (Jia et al. 2002) and has been shown in the case of GSK3β ablation in NSCs that promoted Shh signalling at least via Gli1 (Kim et al. 2009a). In comparison, Notch1 signalling via NICD nuclear activation was reduced dramatically by GSK3β inhibition in the dSVZ compared to the lSVZ, implying a greater role for Notch signalling in regulating oligodendrogenesis and neurogenesis from the dSVZ microdomain. Earlier studies have indicated a direct role for GSK3β in phosphorylating NICD in shortening its half-life (Foltz et al. 2002), whilst KO of GSK3β in NSCs induces the inverse of promoting Notch1 signalling and its target genes in early forebrain development (Kim et al. 2009a). In addition, Notch1 activity is required to be downregulated for the timely differentiation of early OL lineage cells (Wang et al. 1998), which fits with the results of our study where GSK3β inhibition promoted OL lineage progression, as observed previously in the optic nerve (Azim and Butt 2011). BMPs are strong inhibitors of oligodendrogenesis and their downstream TFs work in concert with β-catenin to repress maturation in later stage OL lineage cells (Bilican et al. 2008; Weng et al. 2012). We observed a partial reduction in the downstream BMP pathway factors pSMADs1/5/8 in the dSVZ in response to GSK3β inhibition, which has not previously been reported in the context of SVZ gliogenesis. However, in cultured dorsal spinal cord NPs, FGF2 represses SMADs to induce Olig2 expression (Bilican et al. 2008; Weng et al. 2012). The results indicate GSK3b regulates multiple pathways that to a certain extent are microdomain specific and may have differential roles in regulating oligodendrogenesis and neurogenesis.

Extracellular cues that could regulate OP generation via GSK3β and β-catenin were examined in the dSVZ. Like ARA-014418, Wnt3a was equally effective in modulating GSK3β and β-catenin implicating that GSK3β functions and effects observed are equivalent to the canonical Wnt pathway (Azim et al., 2014). Moreover, FGF2 appears to also regulate GSK3β and β-catenin in the dSVZ, as described in cultured NSCs (Israsena et al. 2004). Intriguingly, EGF and BMP4 almost completely abolished nuclear β-catenin expression, suggesting they may exert an inhibitory effect on endogenous Wnt/β-catenin signalling in the dSVZ. Neurospheres derived from the dorsal embryonic forebrain rapidly lose Wnt-signalling in conditions containing EGF (Machon et al. 2005), and EGF-signalling could repress β-catenin or dorsalising NSC phenotypes.

In summary, these findings are line with our previous study showing GSK3β inhibitors increase the number of OLs and promotes myelination in the developing corpus callosum and following a chemical demyelinating lesion (Azim and Butt 2011). Our present study provides further evidence that postnatally the dSVZ is the primary source of newly generated OLs in the forebrain, and that their generation from NSC/NP is regulated by endogenous GSK3β activity and Wnt signalling in a microdomain specific manner (Azim et al., 2014). The failure of remyelination in MS is due in part due to upregulation of negative regulatory factors and a loss of positive regulatory factors (Franklin and Ffrench-Constant 2008). For example, Notch1 signalling may be upregulated in multiple sclerosis and delay remyelination by inhibiting OPC differentiation (Blanchard et al. 2013; John et al. 2002; Zhang et al. 2009). Targeting GSK3β through the use of small molecule inhibitors may therefore

complement other therapeutic approaches for stimulating OP generation from the dSVZ.

Acknowledgments

References

Adachi K, Mirzadeh Z, Sakaguchi M, Yamashita T, Nikolcheva T, Gotoh Y, Peltz G, Gong L, Kawase T, Alvarez-Buylla A and others. 2007. Beta-catenin signaling promotes proliferation of progenitor cells in the adult mouse subventricular zone. Stem Cells 25:2827-36.

Aguirre A, Gallo V. 2004. Postnatal neurogenesis and gliogenesis in the olfactory bulb from NG2-expressing progenitors of the subventricular zone. J Neurosci 24:10530-41.

Azim K, Butt AM. 2011. GSK3beta negatively regulates oligodendrocyte differentiation and myelination in vivo. GLIA 59:540-53.

Azim K, Fiorelli R, Zweifel S, Hurtado-Chong A, Yoshikawa K, Slomianka L, Raineteau O. 2012a. 3-dimensional examination of the adult mouse subventricular zone reveals lineage-specific microdomains. PLoS ONE 7:e49087.

Azim K, Fischer B, Hurtado-Chong A, Draganova K, Zemke M, Sommer L, Butt AM, RaineteauO. 2014. Persistent Wnt/β-Catenin signaling determines dorsalization of the postnatal subventricular zone and neural stem cell specification into oligodendrocytes and glutamatergic neurons. Stem Cells, in press.

Azim K, Raineteau O, Butt AM. 2012b. Intraventricular injection of FGF-2 promotes generation of oligodendrocyte-lineage cells in the postnatal and adult forebrain. GLIA 60:1977-90.

Bhat R, Xue Y, Berg S, Hellberg S, Ormo M, Nilsson Y, Radesater AC, Jerning E, Markgren PO, Borgegard T and others. 2003. Structural insights and biological effects of glycogen synthase kinase 3-specific inhibitor AR-A014418. J Biol Chem 278:45937-45.

Bilican B, Fiore-Heriche C, Compston A, Allen ND, Chandran S. 2008. Induction of Olig2 precursors by FGF involves BMP signalling blockade at the Smad level. PLoS ONE 3:e2863.

Blanchard B, Heurtaux T, Garcia C, Moll NM, Caillava C, Grandbarbe L, Klosptein A, Kerninon C, Frah M, Coowar D and others. 2013. Tocopherol derivative TFA-12 promotes myelin repair in experimental models of multiple sclerosis. J Neurosci 33:11633-42.

Brill MS, Ninkovic J, Winpenny E, Hodge RD, Ozen I, Yang R, Lepier A, Gascon S, Erdelyi F, Szabo G and others. 2009. Adult generation of glutamatergic olfactory bulb interneurons. Nature Neuroscience 12:1524-33.

Butt AM, Hornby MF, Kirvell S, Berry M. 1997. Platelet-derived growth factor delays oligodendrocyte differentiation and axonal myelination in vivo in the anterior medullary velum of the developing rat. J Neurosci Res 48:588-96.

Cohen P, Goedert M. 2004. GSK3 inhibitors: development and therapeutic potential. Nat Rev Drug Discov 3:479-87.

Doble BW, Woodgett JR. 2003. GSK-3: tricks of the trade for a multi-tasking kinase. J Cell Sci 116:1175-86.

Doetsch F, Caille I, Lim DA, Garcia-Verdugo JM, Alvarez-Buylla A. 1999. Subventricular zone astrocytes are neural stem cells in the adult mammalian brain. Cell 97:703-16.

Doetsch F, Garcia-Verdugo JM, Alvarez-Buylla A. 1997. Cellular composition and three-dimensional organization of the subventricular germinal zone in the adult mammalian brain. J Neurosci 17:5046-61.

Fancy SP, Baranzini SE, Zhao C, Yuk DI, Irvine KA, Kaing S, Sanai N, Franklin RJ, Rowitch DH. 2009. Dysregulation of the Wnt pathway inhibits timely myelination and remyelination in the mammalian CNS. Genes Dev 23:1571-85.

Fei T, Xia K, Li Z, Zhou B, Zhu S, Chen H, Zhang J, Chen Z, Xiao H, Han JD and others. 2010. Genome-wide mapping of SMAD target genes reveals the role of BMP signaling in embryonic stem cell fate determination. Genome Res 20:36-44.

Foltz DR, Santiago MC, Berechid BE, Nye JS. 2002. Glycogen synthase kinase-3beta modulates notch signaling and stability. Curr Biol 12:1006-11.

Franklin RJ, Ffrench-Constant C. 2008. Remyelination in the CNS: from biology to therapy. Nat Rev Neurosci 9:839-55.

Goddard DR, Berry M, Butt AM. 1999. In vivo actions of fibroblast growth factor-2 and insulin-like growth factor-I on oligodendrocyte development and myelination in the central nervous system. J Neurosci Res 57:74-85.

Grimes CA, Jope RS. 2001. The multifaceted roles of glycogen synthase kinase 3beta in cellular signaling. Prog Neurobiol 65:391-426.

He L, Lu QR. 2013. Coordinated control of oligodendrocyte development by extrinsic and intrinsic signaling cues. Neurosci Bull 29:129-43.

Israsena N, Hu M, Fu W, Kan L, Kessler JA. 2004. The presence of FGF2 signaling determines whether beta-catenin exerts effects on proliferation or neuronal differentiation of neural stem cells. Developmental biology 268:220-31.

Jia J, Amanai K, Wang G, Tang J, Wang B, Jiang J. 2002. Shaggy/GSK3 antagonizes Hedgehog signalling by regulating Cubitus interruptus. Nature 416:548-52.

Jiao J, Chen DF. 2008. Induction of neurogenesis in nonconventional neurogenic regions of the adult central nervous system by niche astrocyte-produced signals. Stem Cells 26:1221-30.

John GR, Shankar SL, Shafit-Zagardo B, Massimi A, Lee SC, Raine CS, Brosnan CF. 2002. Multiple sclerosis: re-expression of a developmental pathway that restricts oligodendrocyte maturation. Nat Med 8:1115-21.

Kessaris N, Fogarty M, Iannarelli P, Grist M, Wegner M, Richardson WD. 2006. Competing waves of oligodendrocytes in the forebrain and postnatal elimination of an embryonic lineage. Nat Neurosci 9:173-9.

Kim WY, Snider WD. 2011. Functions of GSK-3 Signaling in Development of the Nervous System. Front Mol Neurosci 4:44.

Kim WY, Wang X, Wu Y, Doble BW, Patel S, Woodgett JR, Snider WD. 2009a. GSK-3 is a master regulator of neural progenitor homeostasis. Nat Neurosci 12:1390-7.

Kim Y, Comte I, Szabo G, Hockberger P, Szele FG. 2009b. Adult mouse subventricular zone stem and progenitor cells are sessile and epidermal growth factor receptor negatively regulates neuroblast migration. PLoS ONE 4:e8122.

Kim YT, Hur EM, Snider WD, Zhou FQ. 2011. Role of GSK3 Signaling in Neuronal Morphogenesis. Front Mol Neurosci 4:48.

Kriks S, Shim JW, Piao J, Ganat YM, Wakeman DR, Xie Z, Carrillo-Reid L, Auyeung G, Antonacci C, Buch A and others. 2011. Dopamine neurons derived from human ES cells efficiently engraft in animal models of Parkinson's disease. Nature 480:547-51.

Lie DC, Colamarino SA, Song HJ, Desire L, Mira H, Consiglio A, Lein ES, Jessberger S, Lansford H, Dearie AR and others. 2005. Wnt signalling regulates adult hippocampal neurogenesis. Nature 437:1370-5.

Machon O, Backman M, Krauss S, Kozmik Z. 2005. The cellular fate of cortical progenitors is not maintained in neurosphere cultures. Mol Cell Neurosci 30:388-97.

Marshall CA, Novitch BG, Goldman JE. 2005. Olig2 directs astrocyte and oligodendrocyte formation in postnatal subventricular zone cells. The Journal of neuroscience : the official journal of the Society for Neuroscience 25:7289-98.

Maurer MH, Bromme JO, Feldmann RE, Jr., Jarve A, Sabouri F, Burgers HF, Schelshorn DW, Kruger C, Schneider A, Kuschinsky W. 2007. Glycogen synthase kinase 3beta (GSK3beta) regulates differentiation and proliferation in neural stem cells from the rat subventricular zone. J Proteome Res 6:1198-208.

Menn B, Garcia-Verdugo JM, Yaschine C, Gonzalez-Perez O, Rowitch D, Alvarez-Buylla A. 2006. Origin of oligodendrocytes in the subventricular zone of the adult brain. The Journal of neuroscience : the official journal of the Society for Neuroscience 26:7907-18.

Nakatani H, Martin E, Hassani H, Clavairoly A, Maire CL, Viadieu A, Kerninon C, Delmasure A, Frah M, Weber M and others. 2013. Ascl1/Mash1 promotes brain oligodendrogenesis during myelination and remyelination. J Neurosci 33:9752-68.

Ortega F, Gascon S, Masserdotti G, Deshpande A, Simon C, Fischer J, Dimou L, Chichung Lie D, Schroeder T, Berninger B. 2013. Oligodendrogliogenic and neurogenic adult subependymal zone neural stem cells constitute distinct lineages and exhibit differential responsiveness to Wnt signalling. Nat Cell Biol.

Ota T, Fujii M, Sugizaki T, Ishii M, Miyazawa K, Aburatani H, Miyazono K. 2002. Targets of transcriptional regulation by two distinct type I receptors for transforming growth factor-beta in human umbilical vein endothelial cells. J Cell Physiol 193:299-318.

Palma V, Lim DA, Dahmane N, Sanchez P, Brionne TC, Herzberg CD, Gitton Y, Carleton A, Alvarez-Buylla A, Ruiz i Altaba A. 2005. Sonic hedgehog controls stem cell behavior in the postnatal and adult brain. Development 132:335-44.

Parras CM, Galli R, Britz O, Soares S, Galichet C, Battiste J, Johnson JE, Nakafuku M, Vescovi A, Guillemot F. 2004. Mash1 specifies neurons and oligodendrocytes in the postnatal brain. EMBO J 23:4495-505. Epub 2004 Oct 21.

Peretto P, Merighi A, Fasolo A, Bonfanti L. 1997. Glial tubes in the rostral migratory stream of the adult rat. Brain Res Bull 42:9-21.

Richardson WD, Kessaris N, Pringle N. 2006. Oligodendrocyte wars. Nat Rev Neurosci 7:11-8.

Smith CM, Luskin MB. 1998. Cell cycle length of olfactory bulb neuronal progenitors in the rostral migratory stream. Dev Dyn 213:220-7.

Wang S, Sdrulla AD, diSibio G, Bush G, Nofziger D, Hicks C, Weinmaster G, Barres BA. 1998. Notch receptor activation inhibits oligodendrocyte differentiation. Neuron 21:63-75.

Weng Q, Chen Y, Wang H, Xu X, Yang B, He Q, Shou W, Higashi Y, van den Berghe V, Seuntjens E and others. 2012. Dual-mode modulation of Smad

signaling by Smad-interacting protein Sip1 is required for myelination in the central nervous system. Neuron 73:713-28.

Wu M, Hernandez M, Shen S, Sabo JK, Kelkar D, Wang J, O'Leary R, Phillips GR, Cate HS, Casaccia P. 2012. Differential modulation of the oligodendrocyte transcriptome by sonic hedgehog and bone morphogenetic protein 4 via opposing effects on histone acetylation. J Neurosci 32:6651-64.

Ye F, Chen Y, Hoang T, Montgomery RL, Zhao XH, Bu H, Hu T, Taketo MM, van Es JH, Clevers H and others. 2009. HDAC1 and HDAC2 regulate oligodendrocyte differentiation by disrupting the beta-catenin-TCF interaction. Nat Neurosci 12:829-38.

Young KM, Fogarty M, Kessaris N, Richardson WD. 2007. Subventricular zone stem cells are heterogeneous with respect to their embryonic origins and neurogenic fates in the adult olfactory bulb. J Neurosci 27:8286-96.

Zhang Y, Argaw AT, Gurfein BT, Zameer A, Snyder BJ, Ge C, Lu QR, Rowitch DH, Raine CS, Brosnan CF and others. 2009. Notch1 signaling plays a role in regulating precursor differentiation during CNS remyelination. Proc Natl Acad Sci U S A 106:19162-7.

Zhou YX, Armstrong RC. 2007. Interaction of fibroblast growth factor 2 (FGF2) and notch signaling components in inhibition of oligodendrocyte progenitor (OP) differentiation. Neurosci Lett 421:27-32.

Figure 1. Functional expression of GSK3β in SVZ microdomains and corpus callosum. (A, B**)** GSK3β expression was measured by qPCR in microdissected microdomains of the P8 SVZ (Azim et al. 2012b) and corpus callosum (CC) at different ages. GAPDH normalised expression values were compared for statistical significance by ANOVA followed by Bonferroni's test. (C-F) Effects of ARA-014418 on GSK3β activity were examined by immunostaining for the inactive form Ser9-pGSK3β in the SVZ microdomains in combination with PI labeling. (G-J) Expression of both Ser9-pGSK3β and the active form Tyr216-pGSK3β in OPs, identified by immunostaining for PDGFRα following ARA-014418 treatment. Arrows in C-F show examples of pronounced endogenous GSK3β activity in the SVZ before (C, E) and after ARA-014418 (D, F).Arrows in G-J indicate increased inactivity in OPs following ARA-014418 infusion (G, H) as well as reduction in the active forms of GSK3β activities within OPs (I, J). (K, L) Western blot analysis of inactive (ser9) pGSK3β and total GSK3β; (L) Data are mean densitometric % changes in values + %SEM (error bars) from *n*>3 replicates (***p<0.01; **p*<0.05). Grey bars represent ARA-014418 and white bars represent controls.

Figure 2. The response of oligodendrocyte lineage cells to ARA-014418 is principally in the dSVZ microdomain. (A, B) Overviews show ARA-014418 induced dramatic increases in the overall density of Sox10+-EGFP+ OL lineage cells dorsally (asterisks); double arrows indicate increased OL cells in the lateral wall of the SVZ. (C-F) Higher magnification shows a profound effect of ARA-014418 on increasing OL lineage cells in the dSVZ microdomain, compared to the lSVZ, where OLs were far less numerous (some indicated by double arrows). Scale bar in B = 100 μm in A, B and scale bar in E = 25 μm in C-F. (G-I) Quantification of Sox10-EGFP+ cells in the dSVZ (G), lSVZ (H) and PVWM (I); data are mean number of cells in a constant volume (FOV), as detailed in methods; error bars represent SEM; *n*≥4 animals (*p<0.05;***p*<0.01; t-test).Grey bars represent ARA-014418 and white bars represent controls.

Figure 3. Inhibition of GSK3β up-regulates markers for NSCs, NPs and OPs predominantly in the dSVZ. Real-time qPCR analysis of the dSVZ microdomain

showing the effects of ARA-014418 on markers for (A) NSCs (ABCG2 and Nestin), (B) NPs (Mash1), and (C) OPs (Olig2 and PDGFRα). Expression was normalised to the house keeping gene GAPDH. White bars are saline/DMSO treated controls and grey bars ARA-014418 treated. Error bars show the SEM (*p<0.05; **p<0.01; t-test).

Figure 4. Inhibition of GSK3β promotes generation of OPs from NSC/NPs of the dSVZ. GSK3β inhibition with ARA-014118 resulted in an increase in the dSVZ of GFAP+ NSC (A, B), Nestin+ NSC/NPs (C, D), and Mash1+ NPs (F, G), and increases the number of Sox10-EGFP+ cells expressing NSC/NP markers (arrows in A-G). Quantification of Sox10-EGFP+ cells co-expressing NSC/NP markers are given in the histograms. (I-K) There was an increase in proliferating OPs within the dSVZ (J, arrows), which was statistically significant (K). Data in E, H, K are mean number of cells in a constant FOV (±SEM), $n \geq 4$ animals per point (**p<0.01, ***p<0.001, t-test), and white bars represent saline/DMSO-treated controls and grey bars ARA-014418 treatment. Scale bar in D = 30 μm in A, B and 20 μm in C, D; scale bar in G = 15 μm in F, G (20 μm in insets); scale bar in J = 20 μm I, J.

Figure 5. Inhibition of GSK3β primarily affects the Wnt-β-catenin pathway in the dSVZ and ISVZ microdomains. (A, B) Cytosolic extracts were assessed for β-catenin and pErk, using β-actin and total Erk as loading controls, respectively (A), and data plotted as mean (±SEM) changes in % densitometric values (B); $n>3$ replicates, **p<0.01, t-test. (C-E) Nuclear extracts were assessed for β-catenin, NICD, pSMAD1/5/8 and Gli1, using H3 as loading control (C), and data plotted as mean (±SEM) changes in % densitometric values (D, E); $n>3$ replicates, **p<0.01, *p<0.05, t-test or ANOVA followed by Bonferroni's posthoc test applied as appropriate. (F) Transcripts known to be induced via Notch, SMAD (TGFβ/BMP) or Wnt-signalling were analysed in the SVZ and data expressed as the mean (±SEM) fold-change of relative expression values, normalised to the housekeeping gene GAPDH; n>3 replicates, *p<0.05; **p<0.01, t-tests. Grey bars represent ARA-014418 and white bars represent controls throughout.

Figure 6. Growth factor specific regulation of GSK3β and β-catenin in the dSVZ. Saline/DMSO, ARA-014418 or a range of growth factors were infused by a single intraventricular infusion into the LV of pups and the dSVZ analysed by western blot. (A, B) Western blots of cytosolic extracts for pGSK3β (vs. total GSK3β) or for nuclear extracts for β-catenin (vs. H3 as internal control). (C, D) Data are expressed as mean ($\pm$SEM) changes in % densitometric values; $n > 3$ replicates, *p<0.05, **p<0.01, ***p<0.001, t-tests vs. control.
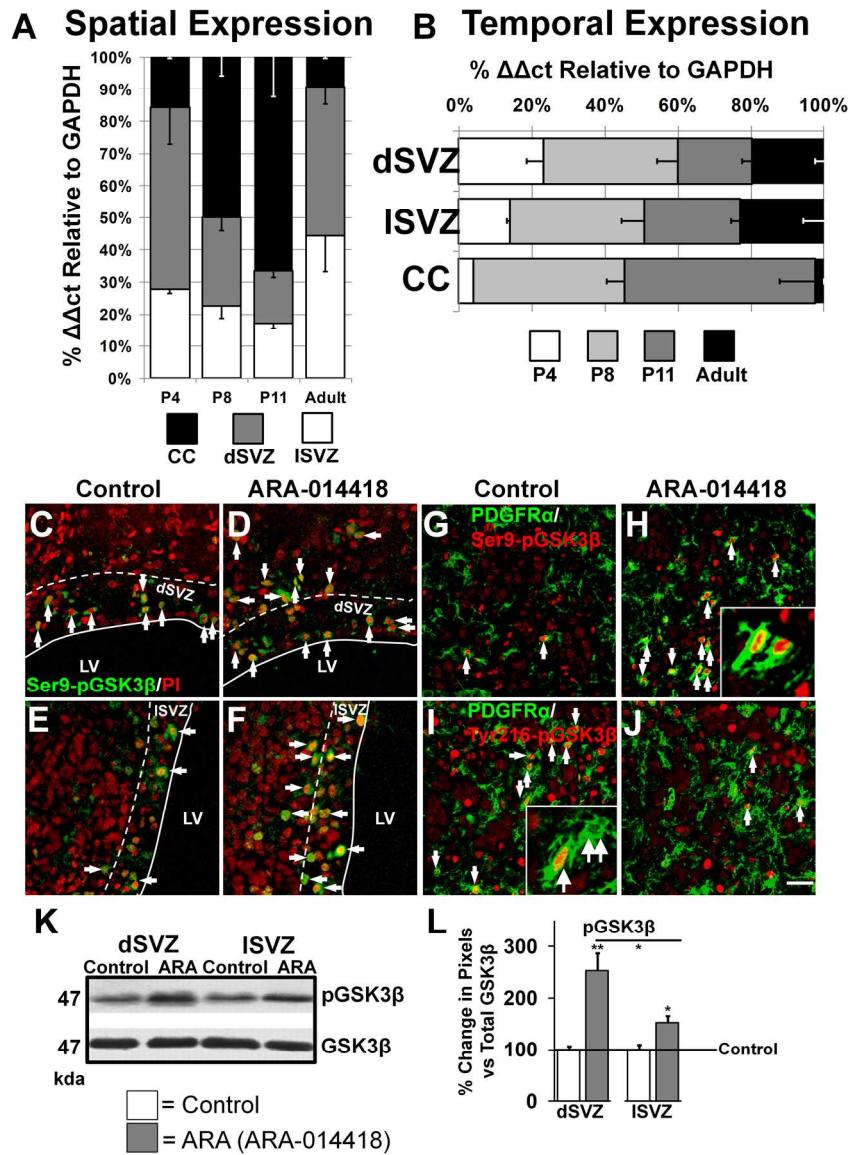
Figure 1
158x219mm (300 x 300 DPI)
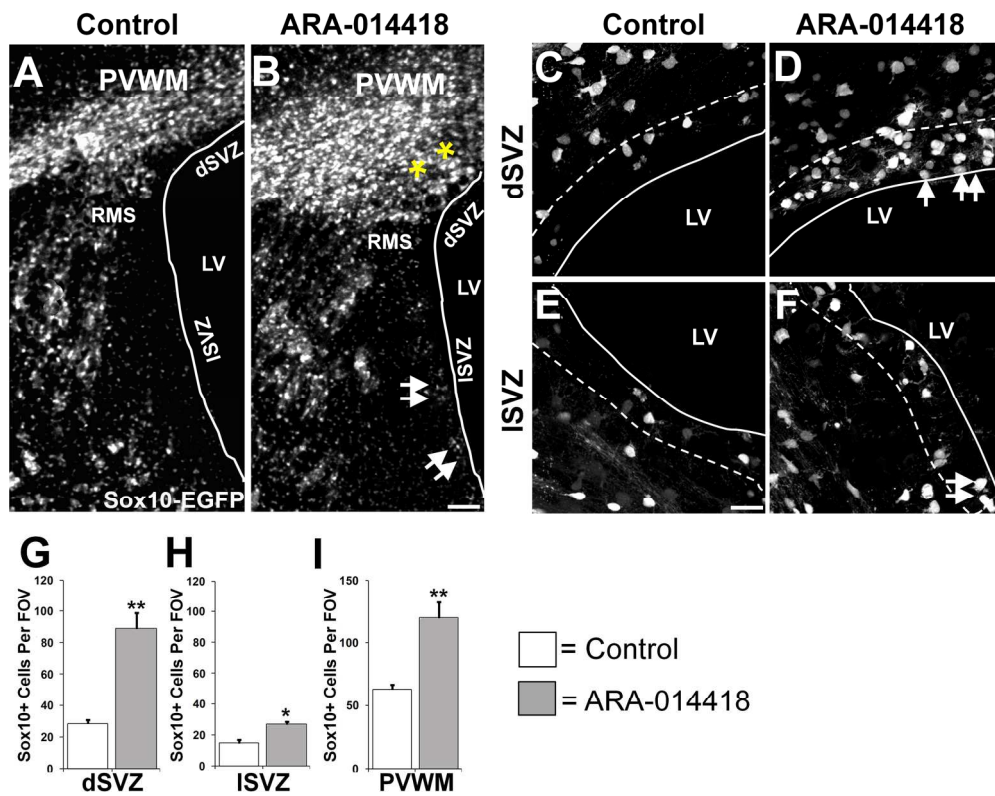
Figure 2
180x144mm (300 x 300 DPI)
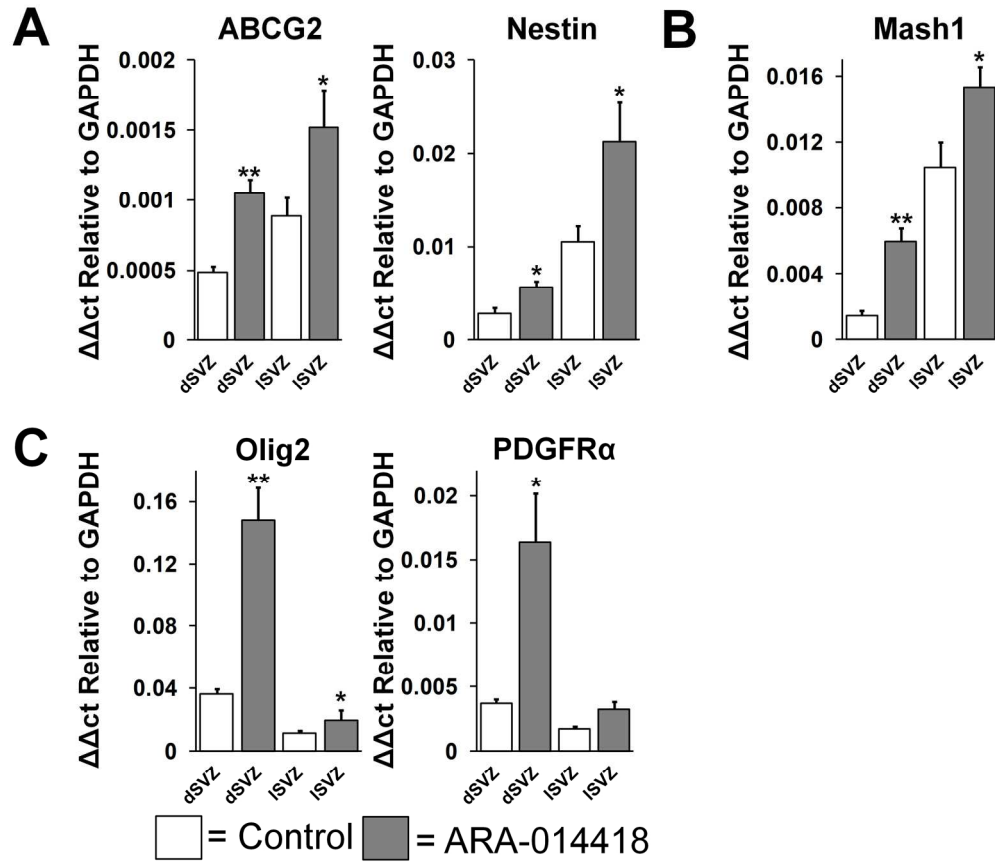
Figure 3
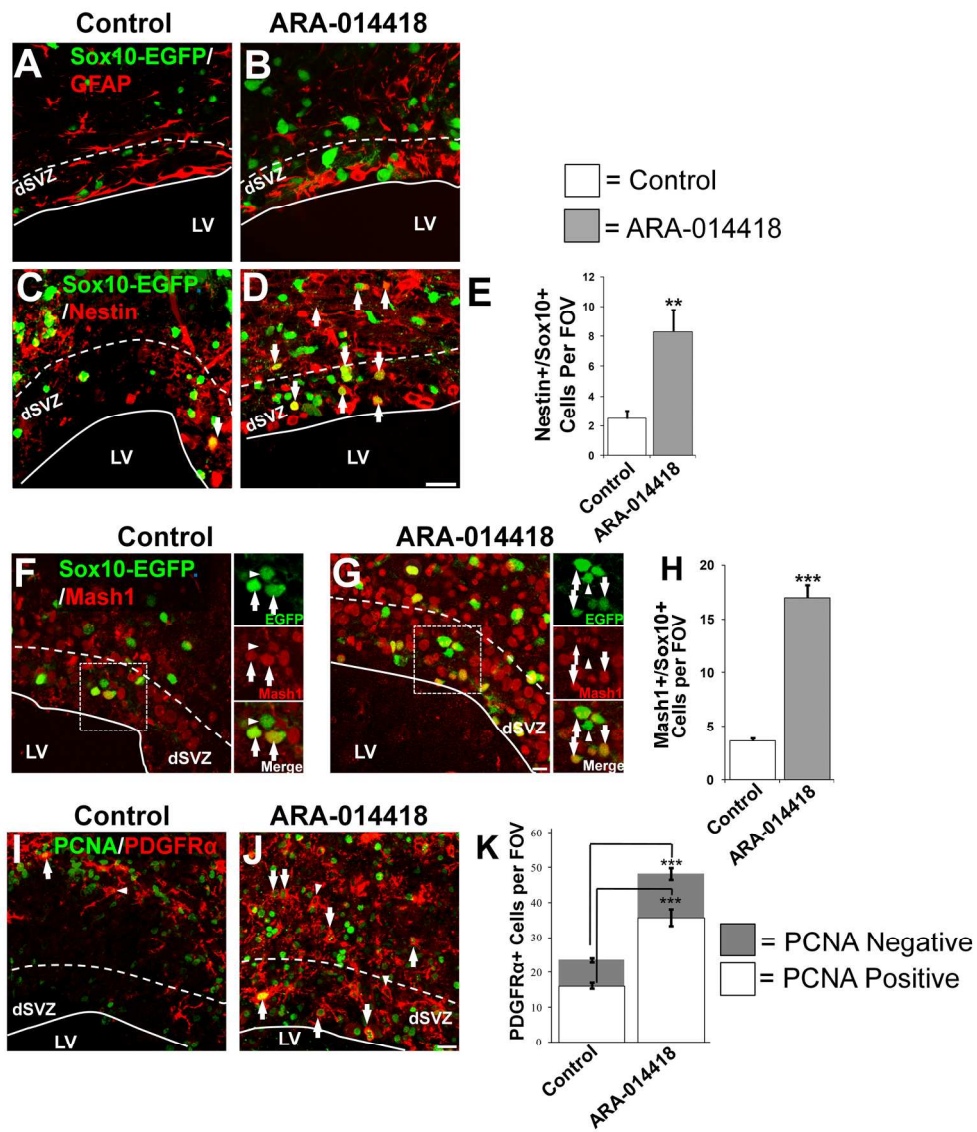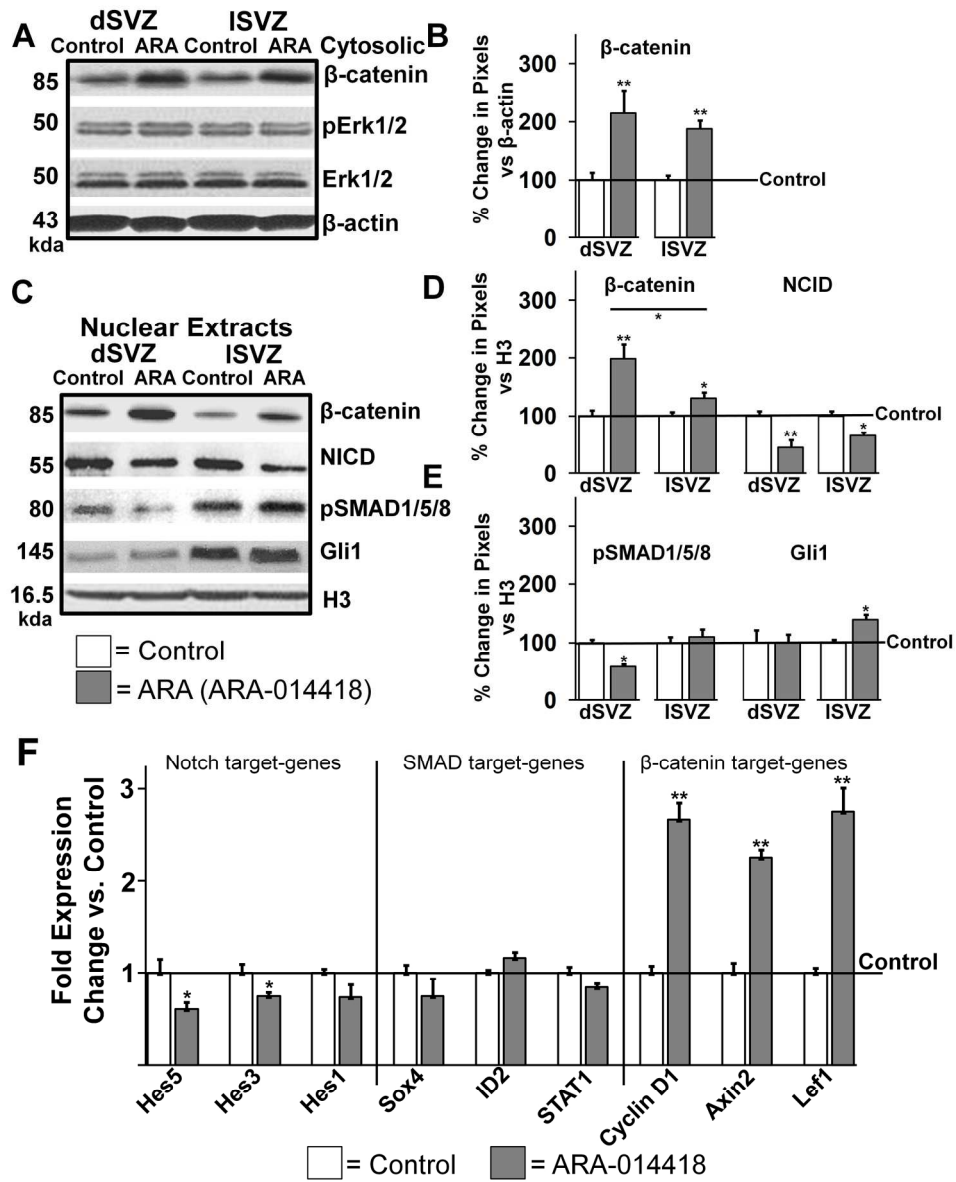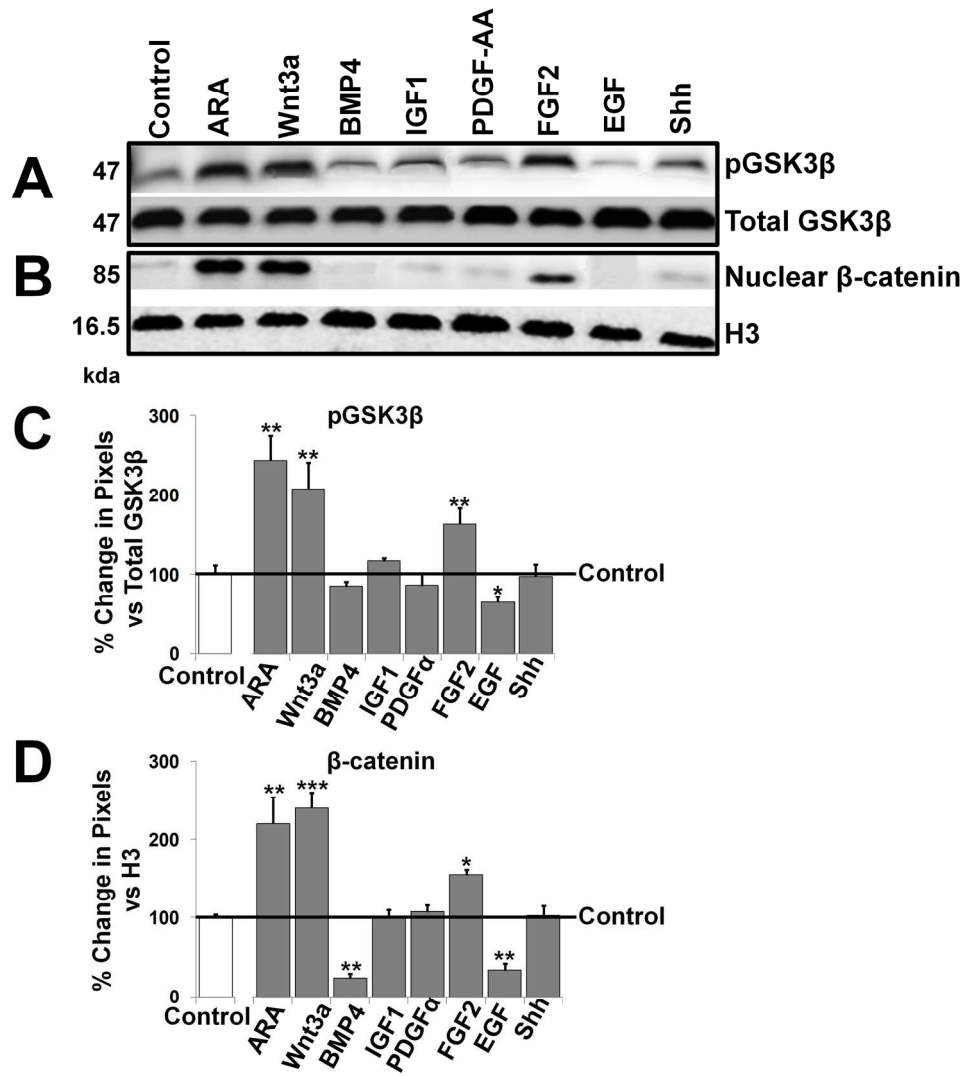180x155mm (300 x 300 DPI)

Figure 4
180x207mm (300 x 300 DPI)

Figure 5
178x219mm (300 x 300 DPI)

Figure 6
180x199mm (300 x 300 DPI)